

CONESCAPANHONDURAS2025paper10.pdf

 Institute of Electrical and Electronics Engineers (IEEE)

Document Details

Submission ID

trn:oid:::14348:477787964

Submission Date

Jul 31, 2025, 11:57 PM CST

Download Date

Aug 1, 2025, 1:08 PM CST

File Name

CONESCAPANHONDURAS2025paper10.pdf

File Size

1.3 MB

6 Pages





3,534 Words

19,694 Characters




21% Overall Similarity

The combined total of all matches, including overlapping sources, for each database.

Match Groups

-  **45 Not Cited or Quoted** 18%
Matches with neither in-text citation nor quotation marks
-  **3 Missing Quotations** 1%
Matches that are still very similar to source material
-  **6 Missing Citation** 3%
Matches that have quotation marks, but no in-text citation
-  **0 Cited and Quoted** 0%
Matches with in-text citation present, but no quotation marks

Top Sources

- 18%  Internet sources
- 18%  Publications
- 0%  Submitted works (Student Papers)

Integrity Flags





0 Integrity Flags for Review

No suspicious text manipulations found.




Our system's algorithms look deeply at a document for any inconsistencies that would set it apart from a normal submission. If we notice something strange, we flag it for you to review.

A Flag is not necessarily an indicator of a problem. However, we'd recommend you focus your attention there for further review.

Match Groups

-  **45 Not Cited or Quoted** 18%
Matches with neither in-text citation nor quotation marks
-  **3 Missing Quotations** 1%
Matches that are still very similar to source material
-  **6 Missing Citation** 3%
Matches that have quotation marks, but no in-text citation
-  **0 Cited and Quoted** 0%
Matches with in-text citation present, but no quotation marks

Top Sources

- 18%  Internet sources
- 18%  Publications
- 0%  Submitted works (Student Papers)

Top Sources

The sources with the highest number of matches within the submission. Overlapping sources will not be displayed.

1	Internet	
arxiv.org		3%
2	Internet	
www.mdpi.com		2%
3	Internet	
ethesis.lib.ku.ac.th		1%
4	Internet	
assets-eu.researchsquare.com		1%
5	Internet	
thesai.org		1%
6	Internet	
repository.uwtsd.ac.uk		1%
7	Internet	
downloads.hindawi.com		<1%
8	Internet	
repositorio.chapingo.edu.mx		<1%
9	Publication	
Thangaprakash Sengodan, Sanjay Misra, M Murugappan. "Advances in Electrical ...		<1%
10	Internet	
oaktrust.library.tamu.edu		<1%

11	Internet	revistatelematica.cujae.edu.cu	<1%
12	Internet	sol.sbc.org.br	<1%
13	Internet	publications.aston.ac.uk	<1%
14	Internet	worldwidescience.org	<1%
15	Internet	arccjournals.com	<1%
16	Publication	Pereira, Filipe Alexandre Sousa. "Development of an Intelligent Computer Vision ...	<1%
17	Internet	heritagesciencejournal.springeropen.com	<1%
18	Publication	ASM Mahmudul Hasan, Dean Diepeveen, Hamid Laga, Michael G.K. Jones, Ferdou...	<1%
19	Publication	Weiyue Xu, Tianyi Wang, Tianyu Ji, Qiong Su, Wei Chen, Changying Ji. "RepGhostC...	<1%
20	Internet	joiv.org	<1%
21	Publication	H.L. Gururaj, Francesco Flammini, S. Srividhya, M.L. Chayadevi, Sheba Selvam. "Co...	<1%
22	Publication	Ajay Kumar, Deepak Dembla, Seema Tinker, Surbhi Bhatia Khan. "Handbook of D...	<1%
23	Publication	Jiajia Li, Kyle Lammers, Xunyu Yan, Xiang Yin, Long He, Jun Sheng, Renfu Lu, Zh...	<1%
24	Publication	V.C. Mahaadevan, R Narayanamoorthi, Sayantan Panda, Sankhaddep Dutta, Gera...	<1%

25	Internet	ebin.pub	<1%
26	Internet	journal2.um.ac.id	<1%
27	Internet	pubs2.ascee.org	<1%
28	Internet	repositorio.espe.edu.ec	<1%
29	Internet	www.biorxiv.org	<1%
30	Internet	www.nature.com	<1%
31	Publication	Ciro Mennella, Umberto Maniscalco, Giuseppe De Pietro, Massimo Esposito. "Adv...	<1%
32	Publication	Das, Shabal. "Advanced Drone Detection: Countering Optical Camouflage Strategi...	<1%
33	Publication	Shi-Hang Cheng, Jun-Zhe Cao. "Hybrid Deep Learning Model for Arch of Aorta Clas...	<1%
34	Publication	Tselios, Dimitrios. "Combining Deep Learning, Handcrafted Features, and Metada...	<1%
35	Publication	Yuanqiu Luo, Jun Sun, Jifeng Shen, Xiaohong Wu, Long Wang, Weidong Zhu. "Appl...	<1%
36	Internet	lml.bas.bg	<1%
37	Internet	www.ijraset.com	<1%
38	Publication	J.L. Del Rosario-Arellano, N.G. Iglesias-Rojas, L.C. Tencos-Muñoz, F.J. Ugalde-Acost...	<1%

39

Publication

"Advanced Network Technologies and Intelligent Computing", Springer Science a... <1%

40

Publication

Xu (Annie) Wang, Julie Tang, Mark Whitty. "Data-centric analysis of on-tree fruit d... <1%

Efficient Optimization of Mango Cultivation Through Image Processing with YOLO and Machine Learning

Abstract—The automatic detection of fruits in agricultural environments represents a key challenge for precision agriculture. This work presents a deep learning-based approach for mango detection in images taken under real field conditions. The YOLOv8 architecture was used as the base model, trained under a supervised scheme, leveraging a custom dataset manually labeled. As part of the preprocessing, classical image enhancement techniques were applied, including resizing to 512×512 pixels and the application of CLAHE (Contrast Limited Adaptive Histogram Equalization) on the luminance channel in the LAB color space, which significantly improved fruit visibility. Multiple trainings were carried out with different configurations, with the YOLOv8x model trained from scratch achieving the best performance. This model reached a precision (P) of 0.752, a recall (R) of 0.905, a mAP@0.5 of 0.795, and a mAP@0.5:0.95 of 0.485. The results demonstrate that the combined use of digital preprocessing and detection based on YOLOv8 enables robust and efficient fruit identification in complex scenarios, laying a solid foundation for future applications in automatic counting, yield estimation, and agricultural robotics.

Index Terms—Mango, climate change, image processing, deep learning, precision agriculture, computer vision.

I. INTRODUCTION

Currently, there is a pursuit for processes to be carried out more efficiently, and agriculture is not exempt from these changes. It is undergoing a significant transformation thanks to the integration of artificial intelligence technologies and deep learning [1]. Real-time and accurate detection of fruits in harvests is crucial for optimizing crop management and planning. In this scenario, the development of increasingly efficient and accurate models for fruit detection has become an area of great interest for many, as the problem is not so simple due to the fact that these fruits are in open environments, which leads to the convergence of many often unpredictable variables, such as environmental factors like wildfires [2] and some pest factors [3]. In the past, these processes were determined empirically and based on observation; however, these methods have a high error rate, as they are inefficient methods.

In Mexico, a study [4] revealed that mango productivity in this region, which is very similar to ours, is influenced by specific edaphoclimatic factors, and the varieties of two types of mangoes seem to benefit more from these climatic conditions. Another factor to consider is the high degree of decomposition that this fruit presents, in which it experiences intense metabolic activity after harvest, limiting its shelf life. In 2017, the journal Food Chemistry [5] conducted a study

in which fruits were treated with chitosan solutions at 0%, 1%, 2%, and 3%, placed in plastic trays and stored at room temperature. Changes in physical and chemical parameters were evaluated to determine the effects of chitosan.

In the field of precision agriculture, deep learning allows, with the help of computational power, the recognition of objects in images through examples, and YOLO models [6] stand out for their speed and accuracy in real-time detection, which makes them very ideal for agricultural applications that require high speed and accuracy. In this regard, we focus on two principles that help us understand the context of this research: MangoYOLO [7], which is a model specifically designed for the efficient detection of mangoes in harvests, with the goal of optimizing crop management and yield estimation; as well as MangoDetNet [8], which is an innovative fruit detection framework that uses weakly supervised learning to be efficient in the use of labels. (Fig. 1).

In El Salvador, recent research has focused on the early detection of diseases in mango production using deep learning approaches [9]. Proposed a CNN-based classification model trained on the MangoFruitDDS dataset, achieving an accuracy of 87.94% using DenseNet201, outperforming other architectures such as MobileNetV2 and ResNet50v2. Their study highlights the potential of convolutional neural networks for addressing pest-related challenges in mango crops, and suggests future implementation on mobile devices or UAVs for large-scale monitoring. In this context, precision models showed better results using YOLO, as it is a real-time object detection model based on deep neural networks. Its main advantage is its speed and accuracy, which makes it ideal for applications where fast processing is required, such as fruit detection, surveillance, autonomous driving, and more. Koirala et al. [7], in their publication, take advantage of this mechanism and execute it perfectly.

By training the model with a specific dataset of mango images, it is possible to develop an efficient system for the automatic detection of mangoes in orchards. This approach improves efficiency in agricultural tasks, such as yield estimation and monitoring the health of the fruits, through the automation of mango detection and counting in real time.

II. MATERIALS AND METHODS

A. Description of the MangoYOLO Dataset

The dataset used in this research is MangoYOLO, a public database developed by Koirala et al. [7], which contains real

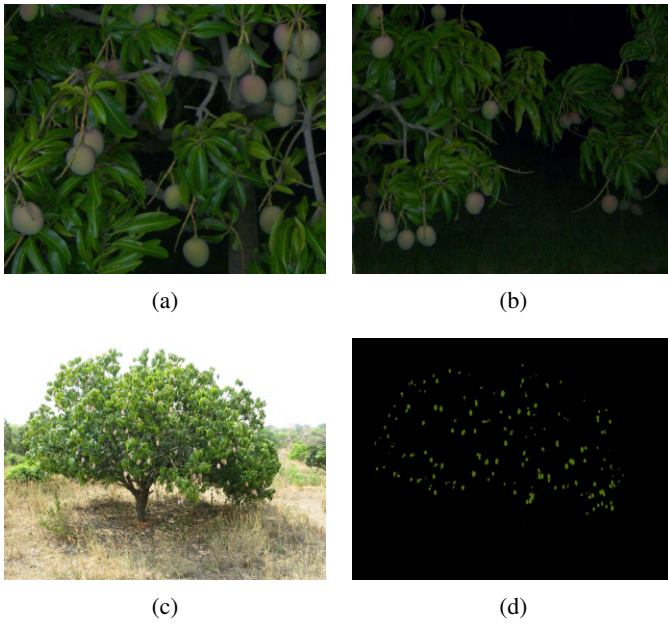


Fig. 1: Dataset used in the training of the MangoYOLO models (a)(b) [7] and MangoDetNet (c)(d) [8].

images of mangoes on trees under variable lighting, occlusion, distance, and fruit ripeness conditions. These characteristics represent a significant challenge for detection models due to the high degree of visual and environmental complexity. The images show green, partially ripe, and ripe mangoes, often occluded by leaves or branches, and photographed under natural or artificial lighting, such as the use of flash. [10]

B. Implementation of Deep Learning Methods

YOLOv8 [11] has an optimized architecture that improves precision compared to YOLOv5, used in MangoYOLO. This is because it uses a better layer structure to extract more detailed features, better handles small objects, which is useful for detecting mangoes of different sizes or on branches, reduces errors in detecting poorly delimited mangoes, detects smaller or partially hidden mangoes with greater accuracy, reduces false positives, and improves automatic counting.

C. Image Preprocessing

In order to improve the visibility of the fruits in the dataset and facilitate future stages of annotation and training, a preprocessing pipeline was designed based on classical digital image processing techniques. This procedure was applied to all images in the original set. As a first step, resizing to 512x512 pixels was performed to standardize the input size. With the image already standardized, CLAHE (Contrast Limited Adaptive Histogram Equalization) [12] was applied to improve local contrast in regions with uneven lighting. (Fig. 2).

This method divides the image into small regions or blocks and applies local histogram equalization with a clipping limit to avoid excessive noise amplification. Afterwards, the blocks are combined using bilinear interpolation to form the final image.



Fig. 2: (a) Original image, (b) Contrast enhancement (CLAHE)

$$\begin{aligned} I_{LAB} &= \text{RGB_to_LAB}(I_{RGB}) \\ L' &= \text{CLAHE}(L) \\ I'_{RGB} &= \text{LAB_to_RGB}(L', A, B) \end{aligned} \quad (1)$$

where I_{RGB} is the original image, I_{LAB} its conversion to LAB space, and L', A, B the channels after applying CLAHE only to the channel L .

This preprocessing significantly improves the visibility of partially hidden fruits or those with uneven lighting, allowing better results to be obtained in subsequent segmentation and automatic detection tasks.

D. Labeling

As an initial result of preprocessing, images with preliminary automatic fruit detection were obtained, generating bounding boxes semi-automatically in YOLO format. However, due to the challenging conditions of the original dataset, such as artificial lighting like the use of flash and the unfavorable location of fruits in numerous images, this method presented significant limitations in the form of false positives. Therefore, it was necessary to carry out an additional stage of manual review and labeling to ensure the precision and quality required in the training of the YOLO model, ensuring robust and reliable results (Fig. 3).

E. Arquitectura de YOLOv8

YOLOv8 se compone de tres partes principales: una red troncal CSPDarknet53 [13] personalizada que extrae características de la imagen; neck con el módulo C2f que fusiona información a múltiples escalas para mejorar la detección, especialmente de objetos pequeños; y head que realiza las predicciones finales de objetos, incluyendo cuadros delimitadores y clases.

F. YOLOv8 Model Training

The YOLOv8 architecture was selected to address mango fruit detection and counting tasks directly on the tree, considering varied environments and lighting conditions. Its structure consists of five functional blocks: input, backbone, neck, head, and output (Fig. 4).

YOLOv8s and YOLOv8m versions were used for their balance between accuracy and speed, which allows their execution on resource-limited devices [14]. These versions



Fig. 3: Example of automatic segmentation. Each green box represents a detected fruit.

implement an efficient backbone and fusion structures such as PANet, facilitating the detection of objects of different sizes, including partially occluded or immature fruits.

G. YOLO Dataset Generation and Annotations

Once preprocessing filters were applied to the MangoYOLO dataset, a new dataset specifically structured for training with the YOLOv8 architecture was generated (Table.I). The enhanced images were used as direct input, and the annotations for YOLO model training were initially generated semi-automatically. Due to false positives, a custom Python script with a graphical interface based on Tkinter was developed, allowing precise and efficient manual bounding box labeling, thereby ensuring the quality and accuracy necessary for effective training and optimal mango detection results. These annotations were then stored in text files using the standard YOLO annotation format (Equation(2)).

$$\langle \text{class} \rangle \langle x_{\text{center}} \rangle \langle y_{\text{center}} \rangle \langle \text{width} \rangle \langle \text{height} \rangle \quad (2)$$

Where all position and size values are normalized with respect to the width and height of the image.

TABLE I: Structure of the dataset generated for YOLOv8

Directory	Content Description
images/train	Preprocessed images for training
images/val	Images for model validation
labels/train	YOLO annotations (.txt) for training
labels/val	YOLO annotations (.txt) for validation

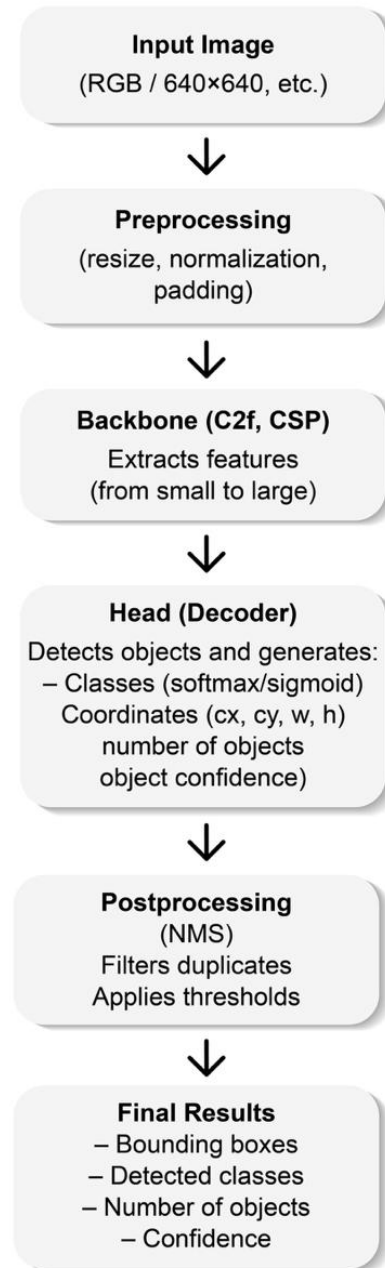


Fig. 4: Functional diagram of the YOLOv8 architecture used in this research.

H. Computational Resources and Experimental Setup

The framework used for training was Ultralytics YOLOv8 (v8.3.141), executed in a *Python 3.11.12* environment on *PyTorch 2.6.0+cu124* with CUDA support enabled. For the development and evaluation of the object detection models proposed in this study, the RunPod platform was used, which allows access to advanced computing resources through dedicated instances.

The three trainings carried out were executed on an NVIDIA RTX 4090 GPU with 24 GB of VRAM, using the Ultralytics YOLOv8 framework (v8.3.145) on *Python 3.10.12* and *Torch 2.1.0+cu118* with CUDA acceleration enabled. The configurations of each training are detailed in Table II, where the model versions used, the number of epochs, and the approaches employed training from scratch, fine-tuning, as well as a lighter version using the YOLOv8m variant are presented.

TABLE II: Configurations used in the trainings

Version	Model	GPU	VRAM	Epochs
v1	YOLOv8x	RTX4090	24 GB	150
v2	YOLOv8x (fine-tuned)	RTX4090	24 GB	150
v3	YOLOv8m	RTX4090	24 GB	150

I. Evaluation Metrics

To evaluate the performance of the models, standard object detection metrics were used: precision, recall, estimated accuracy, and mean Average Precision (mAP). Precision (Equation (3)) measures the proportion of true positives (TP) among all predicted positives. Recall (Equation (4)) indicates the proportion of actual objects that were correctly detected. The F1-score (Equation (5)) is the harmonic mean between precision and recall and is used when a balance between both metrics is desired, especially in contexts with imbalanced classes. Accuracy (Equation (6)), on the other hand, is defined as the proportion of correct predictions, both true positives and true negatives, over the total number of samples. The mAP_{0.5} (Equation (7)) evaluates the average area under the precision-recall curve for each class, using an IoU threshold of 0.5. The mAP_{0.5:0.95} metric (Equation (8)) generalizes the evaluation by averaging mAP across IoU thresholds from 0.5 to 0.95 in increments of 0.05.

$$\text{Precision} = \frac{TP}{TP + FP} \quad (3)$$

$$\text{Recall} = \frac{TP}{TP + FN} \quad (4)$$

$$\text{F1-score} = 2 \cdot \frac{\text{Precision} \cdot \text{Recall}}{\text{Precision} + \text{Recall} + \varepsilon} \quad (5)$$

where ε is a small value to avoid division by zero.

$$\text{Accuracy} = \frac{TP + TN}{TP + FP + FN + TN} \quad (6)$$

$$\text{mAP@0.5} = \frac{1}{N} \sum_{i=1}^N AP_i \quad (7)$$

$$\text{mAP@0.5:0.95} = \frac{1}{10} \sum_{k=0}^9 \text{mAP@IoU=0.5+0.05k} \quad (8)$$

These metrics allow for a detailed and robust evaluation of the model's behavior under real conditions, including partially occluded fruits, diverse lighting, and different levels of ripeness.

(a)



(b)



Fig. 5: (a) Ground truth labels, (b) YOLOv8 predictions

III. RESULTS AND DISCUSSION

During the model evaluation, automatic visualizations of the validation set were generated, allowing a visual comparison of the prediction quality. Figure 5 shows a comparison between the ground truth labels (a) and the predictions generated by the model (b) for the first batch of the validation set. The bounding boxes indicate the location of mangoes in the images.

During the experimentation process, three training sessions were conducted on the RunPod platform, all with an input resolution of 512×512 pixels and a duration of 150 epochs. The first was carried out with the YOLOv8x model from scratch. The second involved a fine-tuning approach, using

the previously trained model as a starting point. In this phase, the initial layers of the convolutional network were frozen to retain the already learned general features, allowing only the final layers to be readjusted specifically to the mango dataset. Additionally, a lower learning rate was used to prevent model overfitting. The third training was executed using the YOLOv8m version, a lighter model optimized to evaluate performance under lower computational consumption. This test allowed a comparison of accuracy and efficiency between different variants of the YOLOv8 architecture.

The best performance was achieved by the first training, with a precision (P) of 0.752, a recall (R) of 0.905, an accuracy of 0.819, a mAP0.5 of 0.795, and a mAP0.5:0.95 of 0.485.

TABLE III: Comparison of YOLOv8 Model Performance Metrics

Metric	v1 (YOLOv8x)	v2 (Fine-tuned)	v3 (YOLOv8m)
Precision (P)	0.752	0.752	0.751
Recall (R)	0.905	0.887	0.913
mAP@0.5	0.795	0.788	0.789
mAP@0.5:0.95	0.485	0.476	0.481
Accuracy	0.819	0.809	0.820

Despite the cost associated with this type of platform, the investment was key to obtaining reproducible results with full control over computational resources, thus enabling prolonged training without interruptions. The results demonstrate that the model succeeds in detecting a high proportion of the objects present in the scene. However, in areas with high fruit density or poor lighting, some false positives and omissions occurred, which explains the moderate value of mAP@0.5:0.95. This comparison (Table III) is fundamental not only for quantitatively evaluating the model's performance but also for visually validating its behavior under real field conditions, thereby strengthening its applicability in precision agriculture environments.

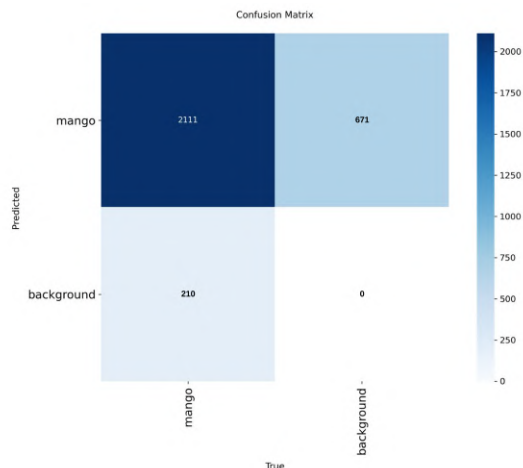


Fig. 6: Confusion matrix of the YOLOv8x model.

Figure 6 illustrates the confusion matrix of the best-performing YOLOv8 model trained for mango detection. This matrix summarizes the relationship between the predicted and actual classes, mango and background. The model correctly detected 2111 mangoes, classified as true positives, while it incorrectly labeled 671 mangoes as background, i.e., false negatives. Additionally, 210 background regions were incorrectly identified as mangoes, i.e., false positives. The remaining values correspond to background areas correctly identified. This configuration reflects a high recall rate, indicating that the model is capable of detecting most mango instances while maintaining reasonable precision.

The observed balance between precision and recall reinforces the model's reliability for agricultural applications in real-world conditions.

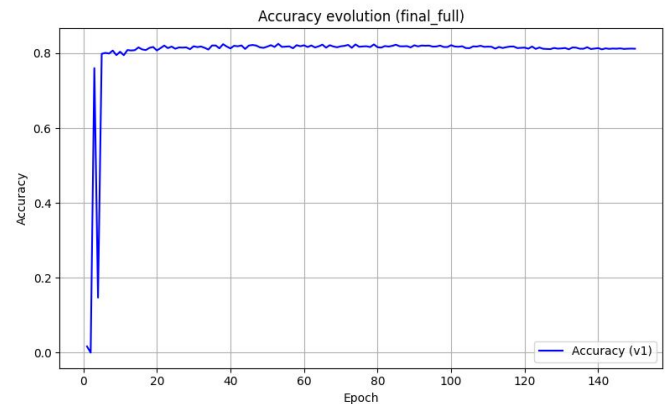


Fig. 7: Accuracy YOLOv8x.

During the training process of model v1, the evolution of performance was recorded over 150 epochs. Figure 7 shows the epoch-by-epoch precision curve, which reveals how the model improves its ability to correctly identify mango instances within the validation set. Precision starts at moderate values and shows a sustained upward trend until it stabilizes near the maximum value. This behavior indicates effective model convergence, validating the consistency of the supervised learning applied to the annotated dataset.

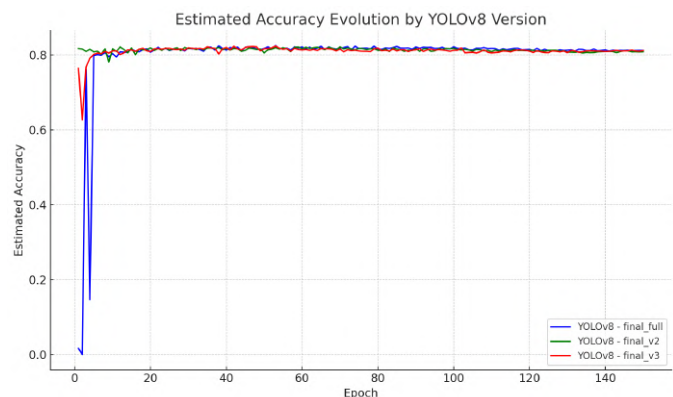


Fig. 8: Comparative Accuracy.

Once the individual performance was analyzed, the results obtained from the three training sessions executed on the same RunPod infrastructure were compared. Figure 8 presents a direct comparison of the estimated accuracy through the curves generated for models v1, v2, and v3. This comparison highlights the differences in stability, learning rate, and final performance among the various configurations used, facilitating the selection of the most suitable model for field applications.

IV. CONCLUSIONS AND FUTURE WORK

This work presented a deep learning-based approach for the automatic detection of mangoes under natural conditions, using the YOLOv8 architecture. Based on a dataset called MangoYOLO, a complete pipeline was developed for annotation, structured organization, and supervised training on real images, addressing challenges such as fruit overlap, partial visibility, and variable lighting conditions.

The results obtained were satisfactory, reaching precisions above 79% and a mAP0.5 of up to 0.745 in the best trained model. In addition, an alternative estimated accuracy metric based on the F1-score was introduced, which is useful in contexts where true negatives are not available, allowing for a more appropriate evaluation of learning.

Among the limitations of the study are the high computational requirements for training complex models, especially on platforms with shared resources such as Google Colab or RunPod. The dependence on precise manual annotations was also identified, representing a time- and effort-intensive task. Likewise, the initial segmentation strategy based exclusively on HSV color filtering showed significant limitations in images with green mangoes or under artificial lighting, generating empty or irrelevant masks.

As future work, it is proposed to integrate advanced data augmentation techniques such as rotation, brightness adjustment, mosaic, and scaling, with the aim of increasing the model's robustness. It is also planned to evaluate lighter variants of the YOLO architecture, aimed at implementation on mobile devices or agricultural drones. Another area of interest is the development of multiclass models that allow distinguishing different degrees of fruit ripeness. Finally, the use of active learning techniques will be explored to optimize sample selection during training, reducing the volume of manually labeled data required.

These advances will enable the proposed solution to scale toward real scenarios of precision agriculture, with applications in automatic counting, harvest estimation, and intelligent crop monitoring.

REFERENCES

- [1] A. González Muñoz *et al.*, "Aplicaciones de técnicas de inteligencia artificial basadas en aprendizaje profundo (deep learning) al análisis y mejora de la eficiencia de procesos industriales," Master's thesis, 2018.
- [2] R. M. Domínguez and D. A. R. Trejo, "Los incendios forestales en México y América Central," in *Memorias del Segundo Simposio Internacional sobre Políticas, Planificación y Economía de los Programas de Protección contra Incendios Forestales: Una visión global*, Albany, California, 2008.
- [3] A. F. Montenegro Bermudez, *Detección y clasificación de antracnosis en mango usando imágenes hiperespectrales y técnicas de aprendizaje profundo*. Doctoral dissertation, Universidad Nacional de Colombia.
- [4] M. Zamudio Galo, R. Serna Lagunes, P. A. Meza, M. E. Galindo Tovar, J. L. Del Rosario Arellano, and J. G. Cruz-Castillo, "Factores edafoclimáticos y productividad de tres variedades de mango (mangifera indica l. cv. palmer) en veracruz, México," *Acta Agronómica*, vol. 72, no. 2, pp. 146–155, 2023.
- [5] G. M. C. Silva, W. B. Silva, D. B. Medeiros, A. R. Salvador, M. H. M. Cordeiro, N. M. da Silva, D. B. Santana, and G. P. Mizobutsi, "The chitosan affects severely the carbon metabolism in mango (mangifera indica l. cv. palmer) fruit during storage," *Food Chemistry*, vol. 237, pp. 372–378, 2017.
- [6] J. Terven, D. M. Córdova-Esparza, and J. A. Romero-González, "A comprehensive review of yolo architectures in computer vision: From yolov1 to yolov8 and yolo-nas," *Machine Learning and Knowledge Extraction*, vol. 5, no. 4, pp. 1680–1716, 2023.
- [7] A. Koirala, K. B. Walsh, Z. Wang, and C. McCarthy, "Deep learning for real-time fruit detection and orchard fruit load estimation: Benchmarking of 'mangoyolo'," *Precision Agriculture*, vol. 20, no. 6, pp. 1107–1135, 2019.
- [8] A. R. Denarda, F. Crocetti, G. Costante, P. Valigi, and M. L. Fravolini, "Mangonetnet: A novel label-efficient weakly supervised fruit detection framework," *Precision Agriculture*, vol. 25, no. 6, pp. 3167–3188, 2024.
- [9] D. R. Santacruz, Y. Rodríguez-Gallo, and C. Rodríguez-Vasquez, "Deep learning-based detection of mango diseases using convolutional neural networks," in *2024 IEEE Central America and Panama Student Conference (CONESCAPAN)*, pp. 1–6, IEEE, 2024.
- [10] J. Redmon and A. Farhadi, "Yolo9000: Better, faster, stronger," in *2017 IEEE Conference on Computer Vision and Pattern Recognition (CVPR)*, pp. 6517–6525, 2017.
- [11] J. F. Jaramillo Hernández, "Aplicación de técnicas de visión artificial en dispositivos de bajo costo para mejorar la eficiencia en la agricultura de precisión," 2023.
- [12] A. M. Reza, "Realization of the contrast limited adaptive histogram equalization (clahe) for real-time image enhancement," *Journal of VLSI signal processing systems for signal, image and video technology*, vol. 38, pp. 35–44, 2004.
- [13] M. Hussain, "Yolo-v1 to yolo-v8, the rise of yolo and its complementary nature toward digital manufacturing and industrial defect detection," *Machines*, vol. 11, no. 7, p. 677, 2023.
- [14] J. Farooq, M. Muaz, K. Khan Jadoon, N. Aafaq, and M. K. A. Khan, "An improved yolov8 for foreign object debris detection with optimized architecture for small objects," *Multimedia Tools and Applications*, vol. 83, no. 21, pp. 60921–60947, 2024.